iScience, Volume *26*

Supplemental information

Continuous population-level monitoring of SARS-CoV-2 seroprevalence in a large European metropolitan region

Marc Emmenegger, Elena De Cecco, David Lamparter, Raphaël P.B. Jacquat, Julien Riou, Dominik Menges, Tala Ballouz, Daniel Ebner, Matthias M. Schneider, Itzel Condado Morales, Berre Doğançay, Jingjing Guo, Anne Wiedmer, Julie Domange, Marigona Imeri, Rita Moos, Chryssa Zografou, Leyla Batkitar, Lidia Madrigal, Dezirae Schneider, Chiara Trevisan, Andres Gonzalez-Guerra, Alessandra Carrella, Irina L. Dubach, Catherine K. Xu, Georg Meisl, Vasilis Kosmoliaptsis, Tomas Malinauskas, Nicola Burgess-Brown, Ray Owens, Stephanie Hatch, Juthathip Mongkolsapaya, Gavin R. Screaton, Katharina Schubert, John D. Huck, Feimei Liu, Florence Pojer, Kelvin Lau, David Hacker, Elsbeth Probst-Müller, Carlo Cervia, Jakob Nilsson, Onur Boyman, Lanja Saleh, Katharina Spanaus, Arnold von Eckardstein, Dominik J. Schaer, Nenad Ban, Ching-Ju Tsai, Jacopo Marino, Gebhard F.X. Schertler, Nadine Ebert, Volker Thiel, Jochen Gottschalk, Beat M. Frey, Regina R. Reimann, Simone Hornemann, Aaron M. Ring, Tuomas P.J. Knowles, Milo A. Puhan, Christian L. Althaus, Ioannis Xenarios, David I. Stuart, and Adriano Aguzzi

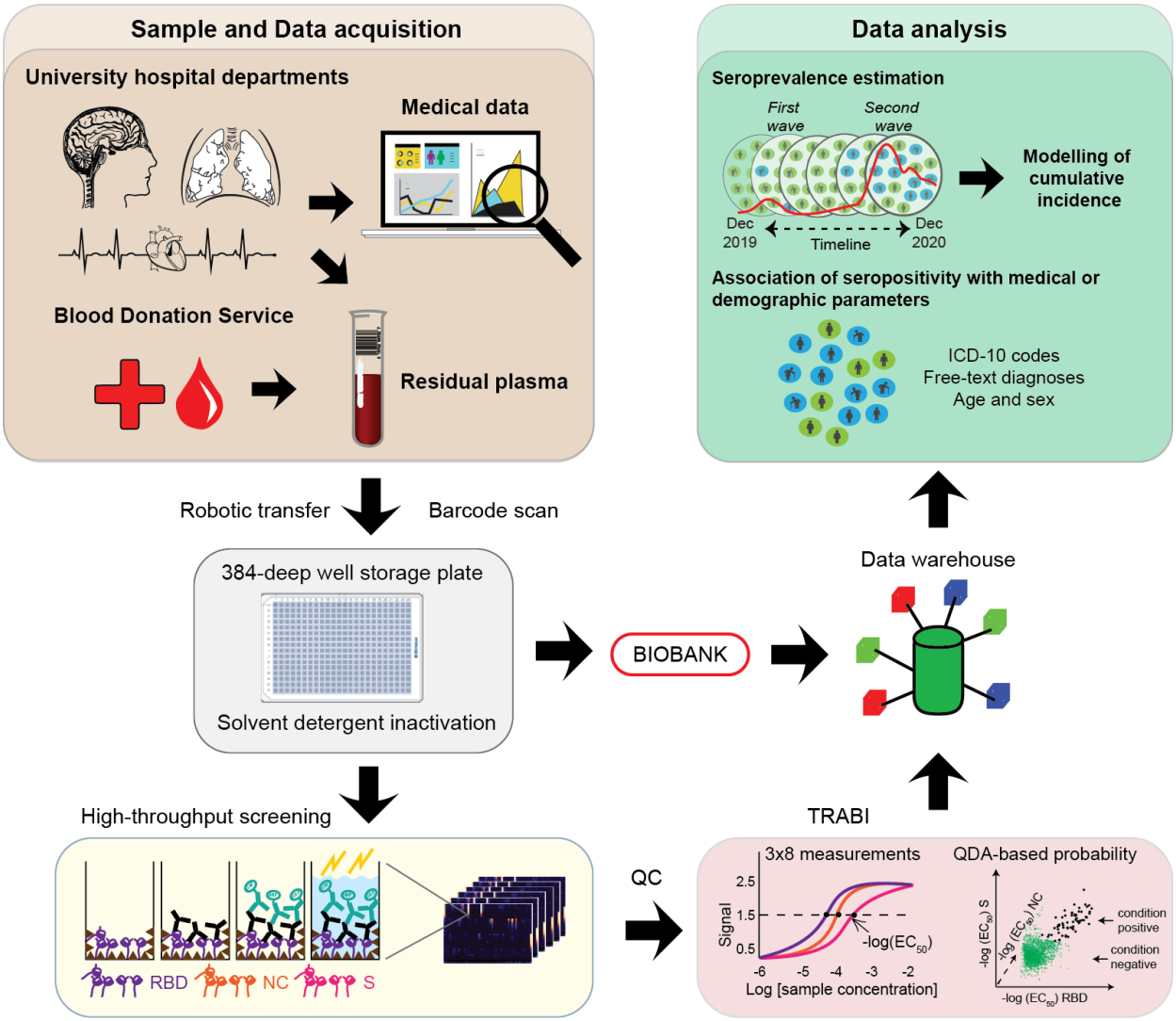

Fig. S1. **Detailed assay procedure, related to Fig. 1A**. Barcoded residual plasma samples from patients admitted to almost all clinical departments of the University Hospital Zurich (USZ) or from healthy donors donating blood to the Blood Donation Services (BDS) Canton Zurich were robotically transferred into 384-deep well plates and subjected to viral inactivation using a solvent detergent procedure. The plates were subsequently stored in a liquid high-throughput biobank, while associated medical data were stored in a custom-designed data warehouse. The samples were used to conduct high-throughput serological assays to interrogate for the presence of antibodies against multiple CoV2 proteins, with an indirect ELISA. To this end, plates were coated with S, RBD, or NC. Following the mapping of ELISA results, antibody titers (i.e. $-\log(EC_{50})$) against the three antigens were determined from eight sample dilutions via logistic regression. The $-\log(EC_{50})$ profiles from both condition negatives (prepandemic samples) and condition positives (convalescent CoV2-PCR-confirmed individuals for BDS and COVID-19 patients for USZ) were used to infer the QDA-based posterior probability of each sample to be seropositive and data was stored in afore mentioned data warehouse. The data was then used for seroprevalence estimation and the modelling of the cumulative incidence. Medical and demographic data was used to interrogate the presence of potential associations between disease and CoV2 positivity.

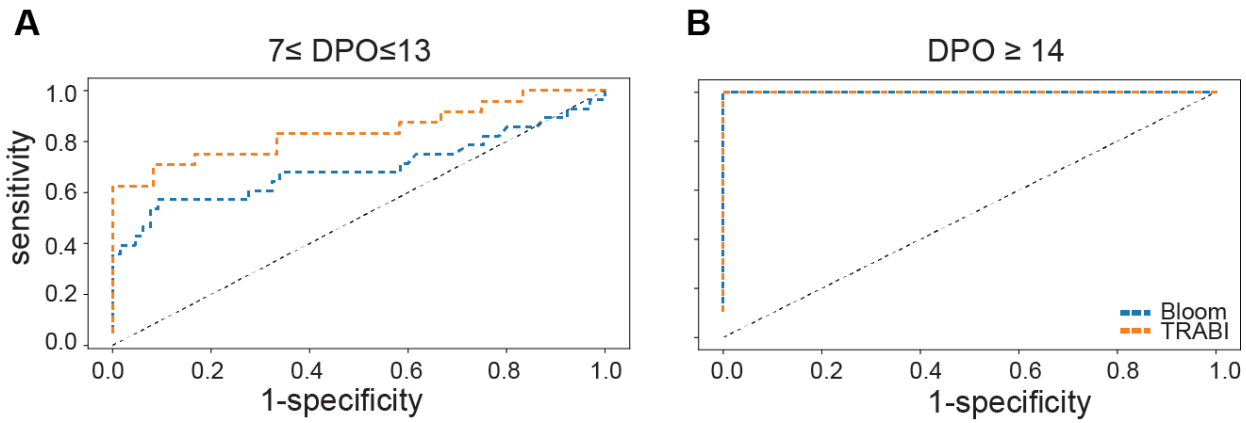

Fig. S2. **Comparison of TRABI to a lateral-flow assay developed by Bloom diagnostics, related to Fig. 1C**. **A**. Comparison between the bloom test and TRABI of samples taken 7 ≤ DPO ≤ 13. **B**. Comparison between the bloom test and TRABI of samples taken DPO ≥ 14.

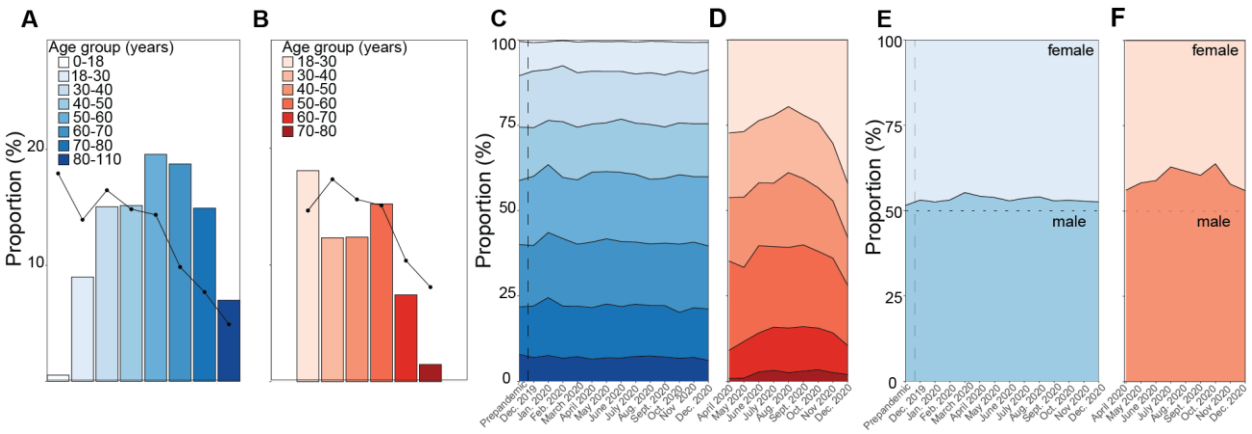

Fig. S3. **Age and sex characteristics of the two cohorts, related to Figs. 2 and 3**. **A** and **B**. Sample distribution according to age groups for USZ (A) and for BDS (B). The age distribution in the USZ sample is quite different from the general population of canton Zürich (black dots). **C** and **D**. Proportion of age groups over time for USZ (C) and for BDS (D). **E** and **F**. Sex distribution over time for USZ (E) and for BDS (F). If there are multiple samples per patient (but never within the same month, as outlined), multiple samples pertaining to the same patient have been included in the analysis.

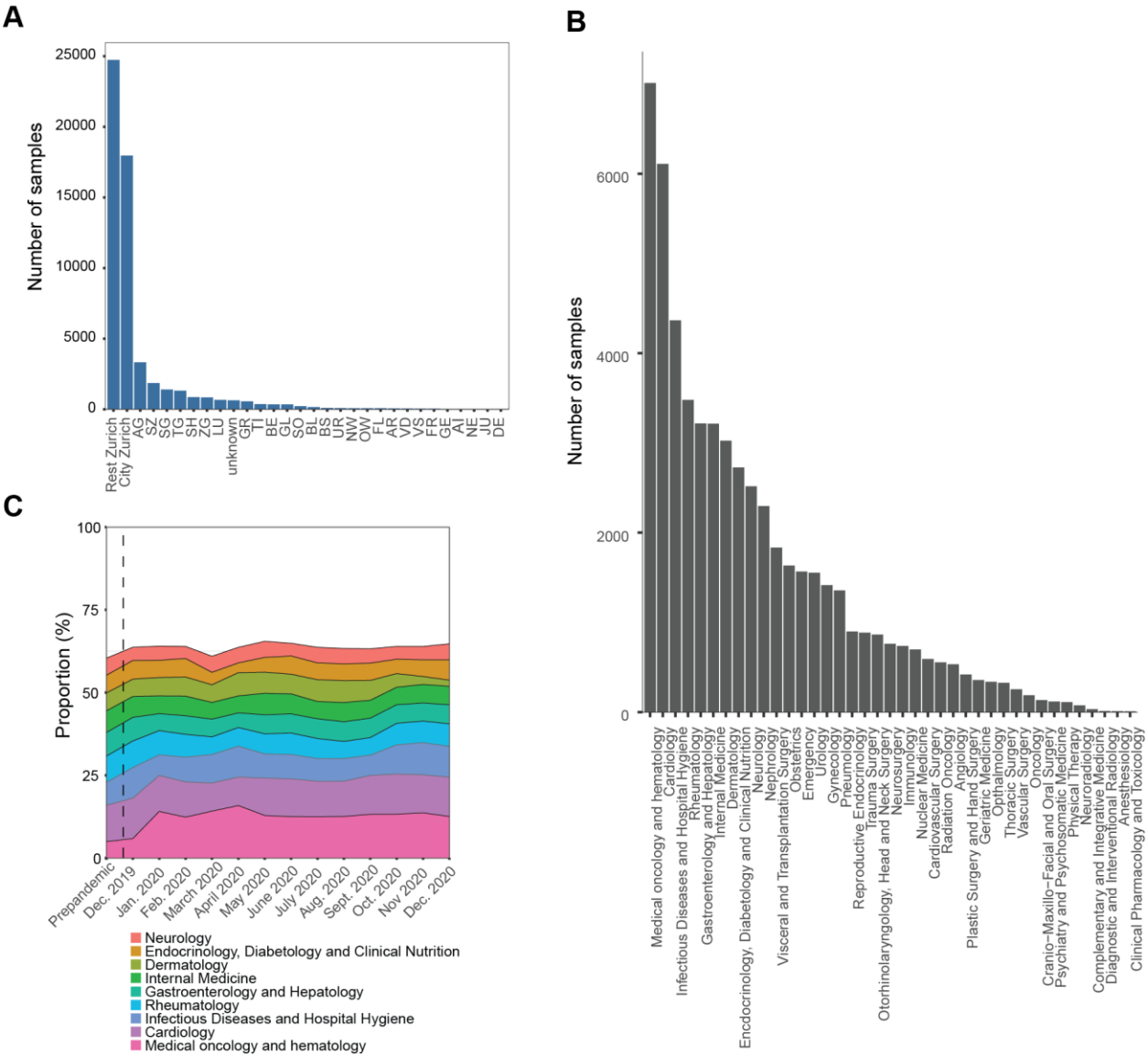

Fig. S4. **Sample provenance and clinical wards of the USZ patients, related to Figs. 2 and 3**. **A**. Sample origin for USZ patients. The two letter codes are official abbreviations of the cantons in Switzerland. Most USZ patients are from the city or from the surroundings of Zurich, followed by the neighbouring cantons. **B**. Clinical departments at which patients were treated. **C**. Distribution of clinical departments over time of study. Except for one department, Medical oncology and hematology, which shows an increase from prepandemic times to January 2020, likely owing to re-structuring of the department, the provenance was stable over time.

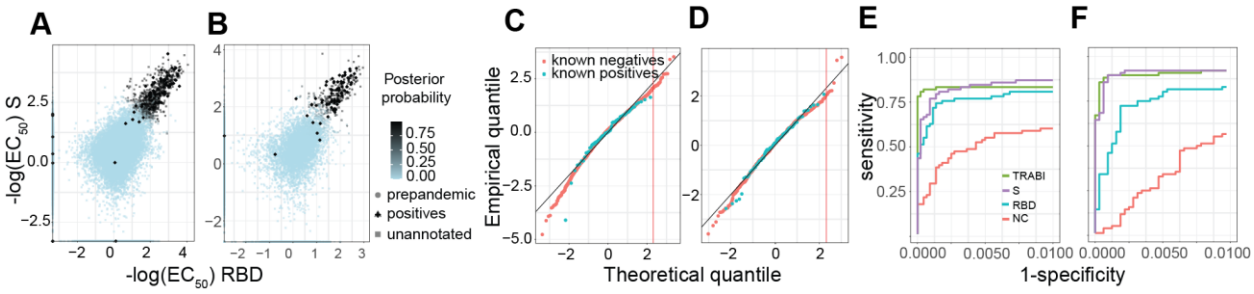

Fig. S5. **Prevalence estimation in two large cohorts, related to Fig. 2**. **A.** and **B**. Depicted are all the –log(EC_{50}) values calculated for S and the RBD for the USZ (A) and the BDS (B) cohort. Posterior probabilities were calculated using LDA. **C**. and. **D**. Q-Q plots to check the Gaussian distributional assumption of the LDA model. For USZ (C) and the BDS (D) cohort respectively, we collapsed the 3 measures per sample according to the linear discriminant classifier. We then scaled known positives and negatives to mean zero and unit variance and compared their distributions to the univariate Gaussian distribution via Q-Q plot. We saw that for the relevant upper tail, the distribution of known negatives followed the normal distribution with only a mild deviation, such that, for instance, the upper one percent quantile is reached at 2.07 (C) and 1.99 (D) rather than at their theoretical value of 2.33. **E**. and. **F**. ROC curves for the USZ (E) and BDS (F) cohorts using the prepandemic samples (including condition negatives from December 2019 and January 2020 for BDS) as condition negatives and selected condition positives from both cohorts.

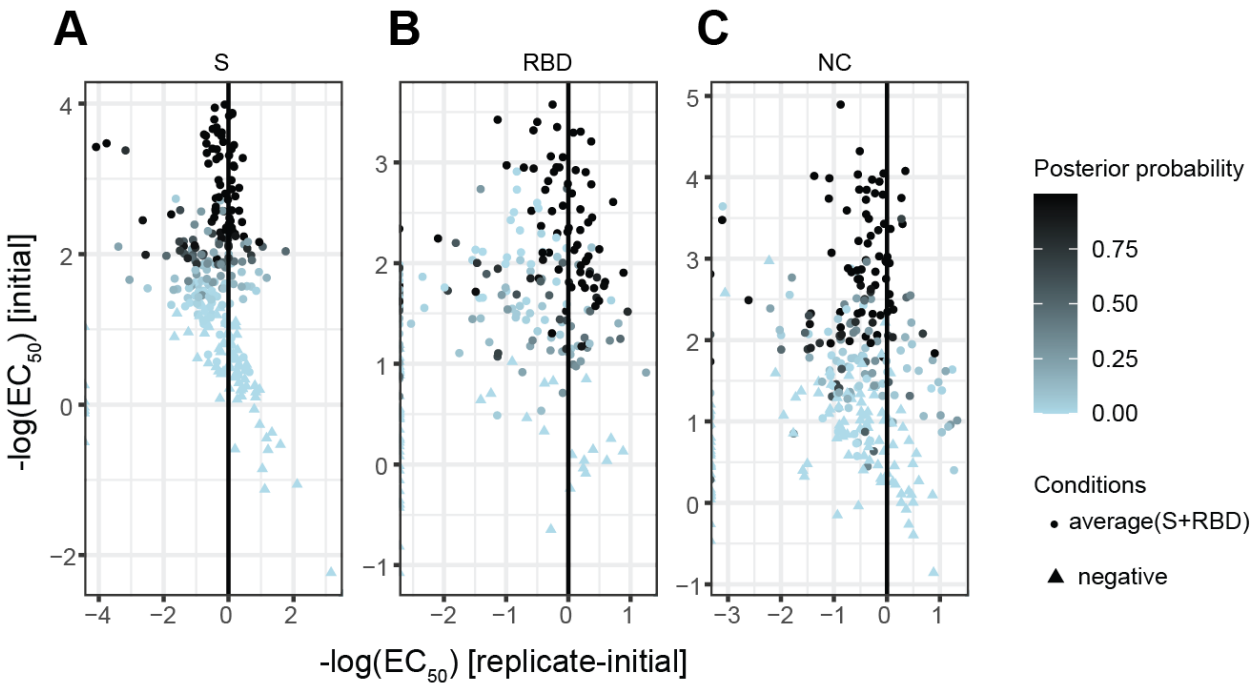

Fig. S6. Assay reproducibility using 210 high scoring samples and 122 random samples (based on results from the high-throughput screen) for binding against S, the RBD, and the NC, related to Figs. 2 and 3. **A.** S binding shows that reproducibility increases at higher values, consistent with increased posterior probabilities. **B.** Same observation as (A) for the RBD. **C**. Same observation as (A) for the NC.

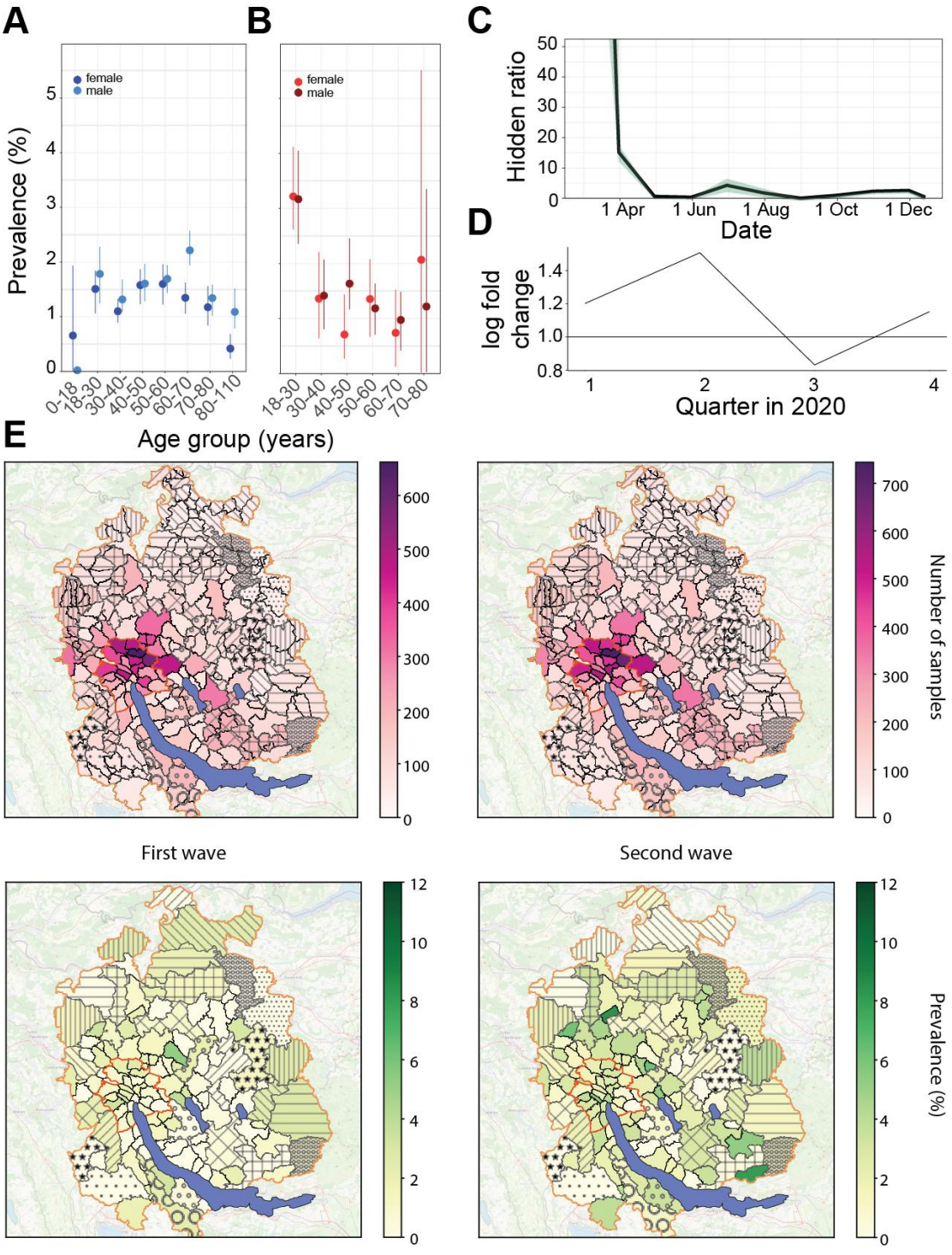

Fig. S7. Epidemiological modelling, related to Figs. 3 and 4. **A**. Seroprevalence according to age and sex for the hospital patients. **B**. Seroprevalence according to age and sex for the blood donors. **C**. Hidden epidemic ratio. **D**. Log fold change of seropositivity of hospital patients from the city versus non-city in four quarters, covering the first and the second wave. **E**. We display the same maps as shown in **Fig. 4** after forming arbitrary groups of zip codes to increase the sample size per region. Hence, we circumvent the need to exclude areas where the total counts were less than 50 patients. The maps display a similar picture as shown in **Fig. 4**, indicating that limiting the analysis to areas with at least 50 patients in total is not posing a representation bias.

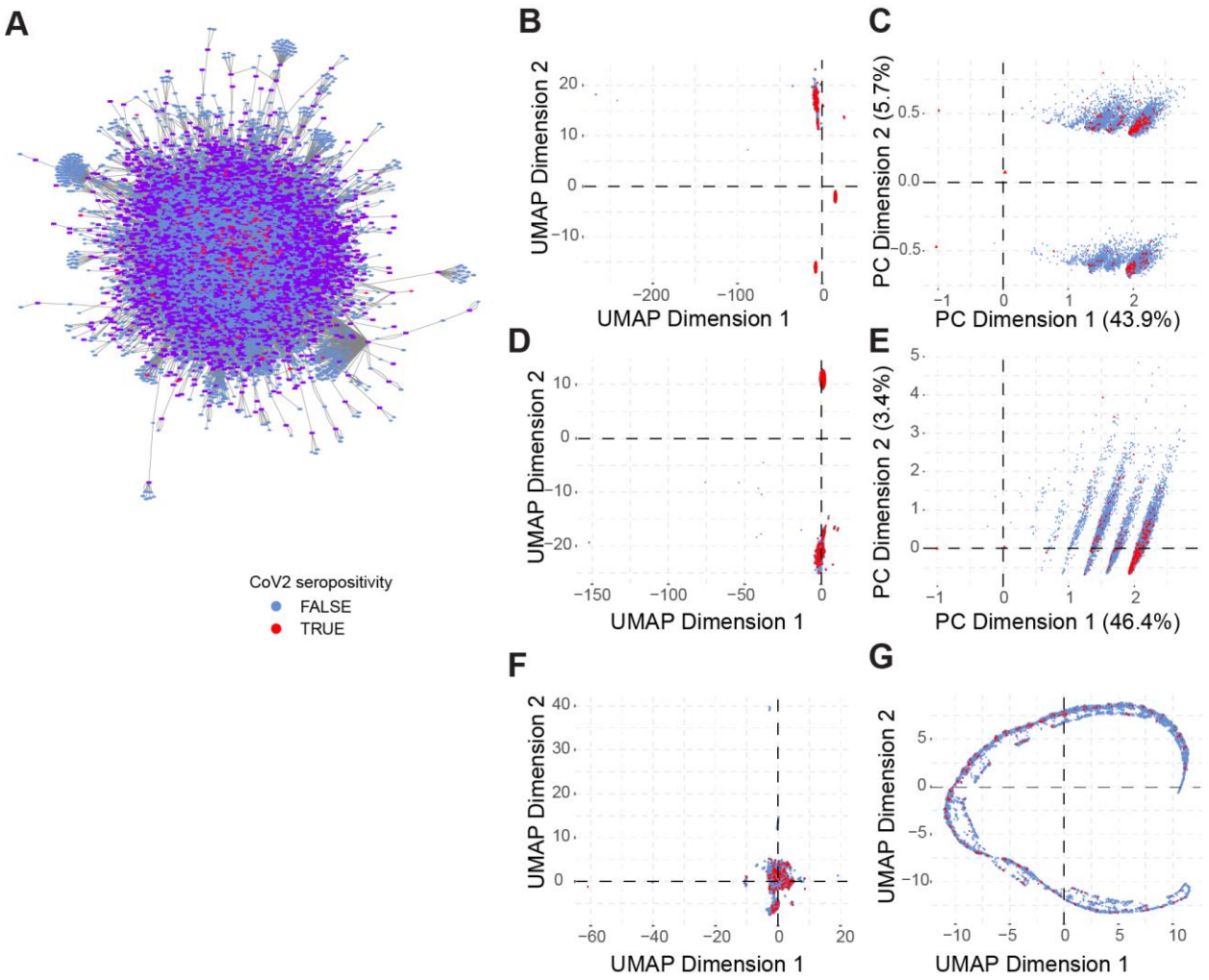

Fig. S8. Exploratory analysis of CoV2 seropositivity with ICD-10 codes and free-text medical reports, related to Fig. 5. **A**. Force directed layout of topological network. ICD-10 codes: purple rectangles. Male patients: diamonds, female patients: circles. Seropositive: red. Seronegative: blue. **B**. Two-dimensional projections of ICD-10 codes as well as female and male sex following UMAP tuned for binary data input using cosine metric. **C**. Principal component analysis of ICD-10 codes as well as female and male sex. **D**. and **E**. Same as in (B) and (C) with exclusion of male/female sex as feature. **F**. and **G**. Representation of dataset with exclusion of patients for which no ICD-10 data exists, using cosine (F) or Euclidean (G) distances. For A-G, seropositivity: red. Seronegativity: blue. No distributional differences between seropositive and seronegative hospital patients were visible.

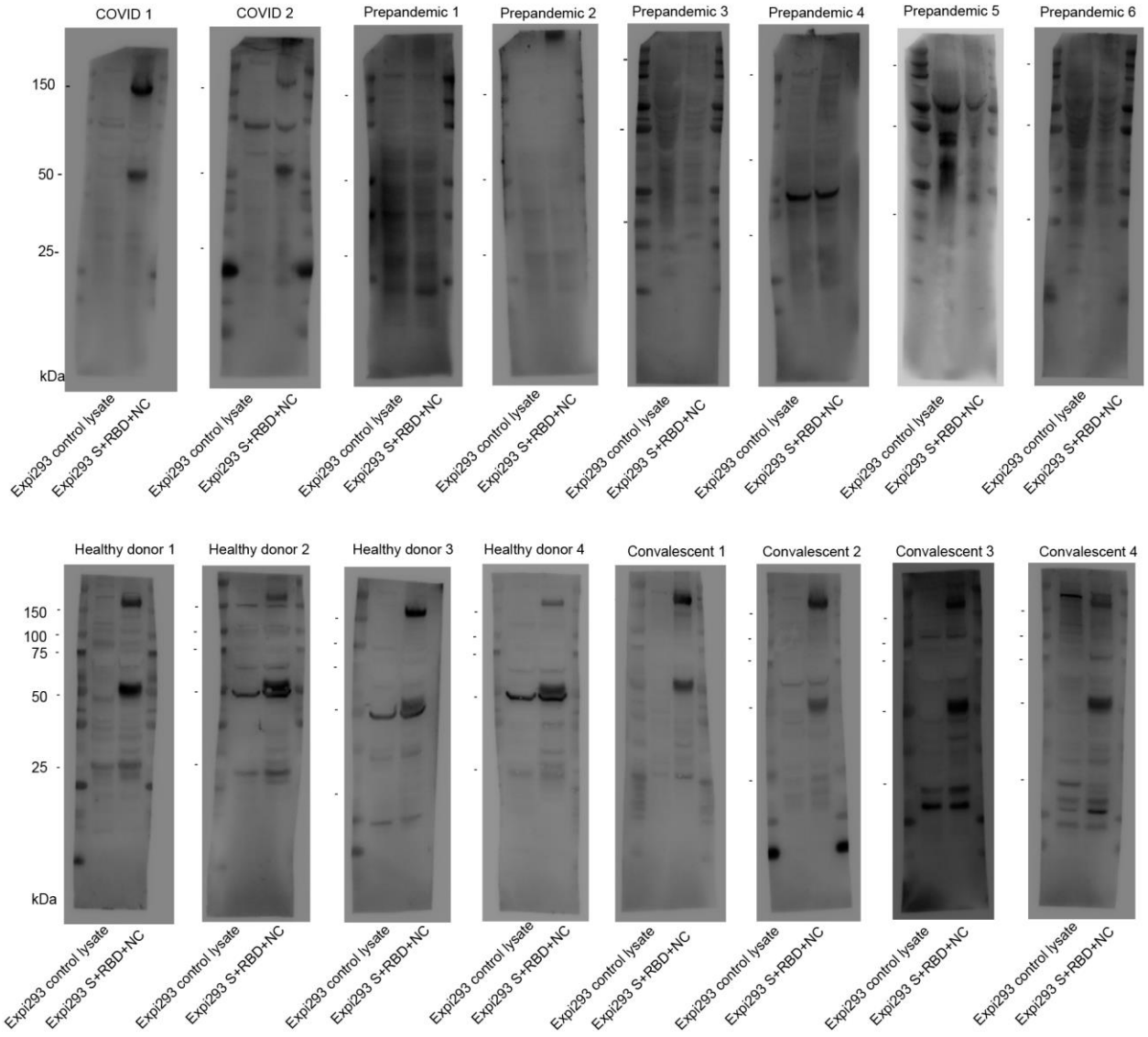

Fig. S9. Uncropped and unmodified camera-acquired images of the Western Blots, related to Figs. 6 and 7.

	Total	No oxygen supply	Oxygen supply	Intubation
Individuals, number	27	8	12	7

Table S1, related to Fig. 1 and Table 1. Characterization of cohort used for assay establishment in terms of disease severity.

ICD-10	ICD-10 Text	Nr. of patients with code
I10.00	Essentielle (primäre) Hypertonie	3251
U99.0	Spezielle Verfahren zur Untersuchung auf SARS-CoV-2	2790
Z11	Spezielle Verfahren zur Untersuchung auf infektiöse und parasitäre Krankheiten	2773
Y84.9	Zwischenfälle durch medizinische Maßnahmen, nicht näher bezeichnet	1756
Z92.1	Dauertherapie (gegenwärtig) mit Antikoagulanzien in der Eigenanamnese	1615
N18.3	Chronische Nierenkrankheit, Stadium 3	1259
I48.0	Vorhofflimmern, paroxysmal	1218
D90	Immunkompromittierung nach Bestrahlung, Chemotherapie und sonstigen immunsuppressiven Maßnahmen	1184
U69.12	Temporäre Blutgerinnungsstörung	1096
B96.2	Escherichia coli [E. coli] und andere Enterobacterales als Ursache von Krankheiten, die in anderen Kapiteln klassifiziert sind	1072
Z86.7	Krankheiten des Kreislaufsystems in der Eigenanamnese	1001
Z95.5	Vorhandensein eines Implantates oder Transplantates nach koronarer Gefäßplastik	992
E11.90	Diabetes mellitus, Typ 2, mit Koma	904
I25.13	Drei-Gefäß-Erkrankung	828
D69.58	Sonstige sekundäre Thrombozytopenien, nicht als transfusionsrefraktär bezeichnet	820
E55.9	Vitamin-D-Mangel, nicht näher bezeichnet	816
E78.4	Sonstige Hyperlipidämien	795
D62	Akute Blutungsanämie	793
Y82.8	Zwischenfälle durch medizintechnische Geräte und Produkte	776
E87.6	Hypokaliämie	734
F05.8	Sonstige Formen des Delirs	722
Y57.9	Komplikationen durch Arzneimittel oder Drogen	711
E03.8	Sonstige näher bezeichnete Hypothyreose	673
I50.01	Rechtsherzinsuffizienz, Sekundäre Rechtsherzinsuffizienz	656
Z92.2	Dauertherapie (gegenwärtig) mit anderen Arzneimitteln in der Eigenanamnese	653
J96.00	Akute respiratorische Insuffizienz, anderenorts nicht klassifiziert	638
I50.12	Linksherzinsuffizienz, Mit Beschwerden bei stärkerer Belastung	629
I25.11	Ein-Gefäß-Erkrankung	619
N39.0	Harnwegsinfektion, Lokalisation nicht näher bezeichnet	614
I25.12	Zwei-Gefäß-Erkrankung	606
X59.9	Sonstiger und nicht näher bezeichneter Unfall	597
D68.4	Erworbener Mangel an Gerinnungsfaktoren	589
N40	Prostatahyperplasie	570
I10.90	Essentielle Hypertonie, nicht näher bezeichnet	566
C43.9	Bösartiges Melanom der Haut, nicht näher bezeichnet	551
E78.8	Sonstige Störungen des Lipoproteinstoffwechsels	547
E87.1	Hypoosmolalität und Hyponatriämie	531
I34.0	Mitralklappeninsuffizienz	526
I11.90	Hypertensive Herzkrankheit ohne (kongestive) Herzinsuffizienz	507
Z95.88	Vorhandensein von sonstigen kardialen oder vaskulären Implantaten oder Transplantaten	504
E11.91	Diabetes mellitus, Typ 2, mit Ketoazidose	493
E83.38	Sonstige Störungen des Phosphorstoffwechsels und der Phosphatase	493
U69.00	Anderenorts klassifizierte, im Krankenhaus erworbene Pneumonie	491
I50.14	Linksherzinsuffizienz, mit Beschwerden in Ruhe	476
I50.13	Linksherzinsuffizienz, mit Beschwerden bei leichterer Belastung	472
D50.8	Sonstige Eisenmangelanämien	467
E78.0	Reine Hypercholesterinämie	455
D64.8	Sonstige näher bezeichnete Anämien	445
J91	Pleuraerguss bei anderenorts klassifizierten Krankheiten	443
A49.8	Sonstige bakterielle Infektionen nicht näher bezeichneter Lokalisation	438

Table S2, related to Table 1 and Fig. 5. 50 most common ICD-10 codes for hospital patients registered in hospital-wide database.

	Seronegative	Seropositive	Overall
Individuals, number	65	71	136
Infected prior to sampling			
Yes	1 (1.6%)	38 (53.5%)	39 (28.9%)
No	63 (98.4%)	33 (46.5%)	96 (71.1%)
Missing	1 (1.5%)	0 (0%)	1 (0.7%)
Infected in 2020			
Yes	3 (10.7%)	42 (80.8%)	45 (56.2%)
No	25 (89.3%)	10 (19.2%)	35 (43.8%)
Missing	37 (56.9%)	19 (26.8%)	56 (41.2%)
Ever infected			
Yes	28 (44.4%)	52 (77.6%)	80 (61.5%)
No	34 (54.0%)	14 (20.9%)	48 (36.9%)
Don't know	1 (1.6%)	1 (1.5%)	2 (1.5%)
Missing	2 (3.1%)	4 (5.6%)	6 (4.4%)
Ever reinfected			
Yes	0 (0.0%)	11 (21.2%)	11 (13.8%)
No	27 (96.4%)	40 (76.9%)	67 (83.8%)
Don't know	1 (3.6%)	1 (1.9%)	2 (2.5%)
Missing	37 (56.9%)	19 (26.8%)	56 (41.2%)

Table S3, related to Fig. 5. Knowledge of infection prior to blood sampling among online health survey participants tested seropositive or seronegative.

	Spring/Summer 2020	Fall/Winter 2020/2021	Winter/Spring 2021/2022	Overall
Individuals, number	12	34	34	80
Symptoms at infection				
Yes	10 (90.9%)	25 (73.5%)	29 (85.3%)	64 (81.0%)
No	1 (9.1%)	9 (26.5%)	5 (14.7%)	15 (19.0%)
Missing	1 (8.3%)	0 (0%)	0 (0%)	1 (1.3%)
Hospitalisation due to COVID-19				
Yes	5 (41.7%)	8 (23.5%)	1 (2.9%)	14 (17.5%)
No	7 (58.3%)	26 (76.5%)	33 (97.1%)	66 (82.5%)
Oxygen supplementation				
Yes	4 (80.0%)	6 (75.0%)	1 (100.0%)	11 (78.6%)
No	1 (20.0%)	2 (25.0%)	0 (0.0%)	3 (21.4%)
Missing	7 (58.3%)	26 (76.5%)	33 (97.1%)	66 (82.5%)
Intensive care treatment				
Yes	4 (80.0%)	3 (37.5%)	1 (100.0%)	8 (57.1%)
No	1 (20.0%)	5 (62.5%)	0 (0.0%)	6 (42.9%)
Missing	7 (58.3%)	26 (76.5%)	33 (97.1%)	66 (82.5%)
Mechanical ventilation				
Yes	2 (50.0%)	3 (100.0%)	1 (100.0%)	6 (75.0%)
No	2 (50.0%)	0 (0.0%)	0 (0.0%)	2 (25.0%)
Missing	8 (66.7%)	31 (91.2%)	33 (97.1%)	72 (90.0%)
Diagnosed pneumonia				
Yes	3 (25.0%)	5 (15.2%)	1 (3.0%)	9 (11.5%)
No	8 (66.7%)	28 (84.8%)	29 (87.9%)	65 (83.3%)
Don't know	1 (8.3%)	0 (0.0%)	3 (9.1%)	4 (5.1%)
Missing	0 (0%)	1 (2.9%)	1 (2.9%)	2 (2.5%)

Table S4, related to Fig. 5. Severity of infection among online health survey participants reporting a known CoV2 infection up to April/May 2022, stratified by infection wave.

	Never infected	Infected	Overall
Individuals, number	50	80	136
EQ-5D-5L score			
Mean (SD)	0.81 (0.17)	0.87 (0.19)	0.85 (0.18)
Median (IQR)	0.85 (0.74 to 1.00)	0.91 (0.83 to 1.00)	0.89 (0.79 to 1.00)
Range	0.42 to 1.00	-0.02 to 1.00	-0.02 to 1.00
Missing	5 (10.0%)	11 (13.8%)	20 (14.7%)
EQ VAS score			
Mean (SD)	70.30 (20.88)	75.00 (15.83)	72.92 (18.18)
Median (IQR)	74.50 (60.75 to 89.50)	78.50 (70.25 to 84.75)	76.00 (70.00 to 85.00)
Range	18.00 to 97.00	10.00 to 100.00	10.00 to 100.00
Missing	4 (8.0%)	10 (12.5%)	18 (13.2%)

Table S5, related to Fig. 5. Health status measured by EQ-5D-5L and EQ VAS among online health survey participants reporting a known CoV2 infection up to April/May 2022.